Confidential Information:	Revised manuscript re-submitted to FEMS Microbiology Ecology

Progressive biogeochemical transformation of placer gold particles drives compositional changes in associated biofilm communities

Maria Angelica Rea[1,2], Christopher D. Standish[3], Jeremiah Shuster[1,2], Andrew Bissett[4], Frank Reith[1,2*]

Affiliations:

[1]The University of Adelaide, School of Biological Sciences, Department of Molecular and Cellular Biology, Adelaide, South Australia 5005, Australia

[2]CSIRO Land and Water, Environmental Contaminant Mitigation and Technologies, PMB2, Glen Osmond, South Australia 5064, Australia

[3]Department of Archaeology, University of Southampton, Southampton, SO17 1BF, UK

[4]CSIRO Oceans and Atmosphere, Battery Point, Tasmania 7005 Australia

Running title: Biogeochemical transformation of gold from the UK

Keywords: Gold, bacteria, biofilms, biogeochemistry, diversity, adaptation, NGS

Number of Pages: 34

Number of Figures: 9

Number of Tables: 1

*Corresponding author:

A/Prof. Frank Reith, Dr. Jeremiah Shuster, Maria Angelica Rea

Department of Molecular and Cellular Biology, School Biological Sciences, The University of Adelaide

i. *CURRENT ADDRESS:*

ii. *CSIRO Land and Water*

PMB 2

Glen Osmond, 5064

South Australia, Australia

iii. *PHONE:* *+61 8 8303 8469*

iv. *FAX:* *+61 8 8303 8550*

E-MAIL: Frank.Reith@csiro.au

jeremiah.shuster@adelaide.edu.au

angel.rea@adelaide.edu.au

Abstract

Biofilms on placer gold (Au)-particle surfaces drive Au solubilization and re-concentration thereby progressively transforming the particles. Gold solubilization induces Au-toxicity; however, Au-detoxifying community members ameliorates Au-toxicity by precipitating soluble Au to metallic Au. We hypothesize that Au-dissolution and re-concentration (precipitation) places selective pressures on associated microbial communities, leading to compositional changes and subsequent Au-particle transformation. We analyzed Au-particles from eight United Kingdom sites using next generation sequencing, electron microscopy and micro-analyses. Gold particles contained biofilms composed of prokaryotic cells and extracellular polymeric substances intermixed with (bio)minerals. Across all sites communities were dominated by Proteobacteria (689, 97% Operational Taxonomic Units, 59.3% of total reads), with β-Proteobacteria being the most abundant. A wide range of Au-morphotypes including nanoparticles, micro-crystals, sheet-like Au and secondary rims, indicated that dissolution and re-precipitation occurred, and from this transformation indices were calculated. Multivariate statistical analyses showed a significant relationship between the extent of Au-particle transformation and biofilm community composition, with putative metal-resistant Au-cycling taxa linked to progressive Au transformation. These included the genera *Pseudomonas, Leptothrix* and *Acinetobacter.* Additionally, putative exoelectrogenic genera *Rhodoferax* and *Geobacter* were highly abundant. In conclusion, biogeochemical Au-cycling and Au-particle transformation occurred at all sites and exerted a strong influence on biofilm community composition.

KEY WORDS: gold, bacteria, biofilms, biogeochemistry, diversity, adaptation, NGS

1. INTRODUCTION

Gold (Au) biogeochemical cycling involves Au solubilization and re-concentration/precipitation processes which contribute to the transformation of placer Au-particles (commonly known as Au grains and nuggets). These processes are mediated, in part, by biofilms occurring on the surface of Au-particles (Southam et al. 2009; Reith et al. 2013). It has been demonstrated that Au solubilization can occur in the presence of reactive Mn-oxide minerals such as birnessite. This mineral, in the presence of a Au-complexing ligand, is capable of oxidizing Au(0) and Au(I) to Au(III) complexes (Ta et al. 2014, 2015). Many microbes produce Au-complexing ligands, *e.g.*, organic acids, thiosulfate and cyanide, that stabilize Au in solution (Reith et al. 2007; Fairbrother et al. 2009; Shuster et al. 2014). These Au(I/III) complexes are highly cytotoxic as they exert oxidative stress in a similar manner as Ag(I)- and Hg(II)-compounds (Nies 1999). Some bacteria, from biofilms on placer Au particle surfaces, have developed biochemical responses to cope with Au toxicity by reducing Au(I/III) complexes resulting in the formation of Au(0) nanoparticles (Checa et al. 2007; Reith et al. 2009; Johnston et al. 2013; Wiesemann et al. 2013, 2017). These Au nanoparticles exhibit a range of morphologies including triangular, spherical, hexagonal and octahedral crystals, and structures that are bacteriomorphic, sheet-like and wire-like. Primary Au particles often contain cores comprised of both Au and Ag; this Au-Ag alloy composition is indicative of the particles' (high temperature) origin. Accumulation of secondary Au structures on the outer surface of primary Au particles can lead to the formation of pure, *i.e.*, >99 wt. %, Au rims (Reith et al. 2010, 2013; Shuster et al. 2015). The Au-enriched rims can range from a few micrometers to several hundred micrometers in thickness. Typically, they contain a nano- and micro-crystalline fabric and are attributed, in part,

to biogeochemical Au/Ag dissolution and Au re-precipitation processes that occurs under near-surface conditions (*e.g*., Fairbrother et al. 2012; Reith, Stewart and Wakelin 2012; Shuster et al. 2017a; Stewart et al. 2017). The extent to which these processes influence the formation of these rims depends on environmental conditions since accretionary and detrital processes can produce similar morphotypes (Groen, Craig and Rimstidt 1990; McCready, Parnell and Castro et al. 2003; Fairbrother et al. 2012; Reith, Stewart and Wakelin 2012; Craw and Lilly 2016; Stewart et al. 2017).

Biofilms are known to adapt when exposed to elevated concentrations of heavy metals (*e.g*., Golby et al. 2014; Koechler et al. 2015). In the context of metal resistance adaptation on a field scale, microbial communities within soils overlying Au-bearing deposits have been shown to have assemblages that are significantly different to that of communities from soils that are distal from deposits (Reith et al. 2012, 2015; Wakelin et al. 2012). Microbial communities above deposits were enriched in functional genes that enabled heavy metal detoxification; furthermore, the greater enrichment of these genes corresponded with Au deposits that experienced prolonged periods of weathering (Reith et al. 2012, 2015). Changes in biofilm compositions have also been observed on a localized scale, *i.e.*, on Au particle surfaces. In the study by Rea et al. (2016), microorganisms directly occurring on the surface of Australian, New Zealand and Brazilian placer Au particles were classified into six functional groups based on a range of operational taxonomic units (OTUs). Group one includes organisms such as *Arthrobacter* spp. and *Staphylococcus* spp. that are important for Au particle surface conditioning, microbial attachment, and biofilm establishment. Group two taxa contribute to the production of extracellular polymeric substances (EPS) and auto-aggregation, and include *Pseudomonas* spp., and *Rhodobacter* spp. Group three microbes affect nutrient cycling*, i.e*., C and N cycling, and include *Sphingobium* sp., *Corynebacterium* sp.*,* and *Acidovorax* spp. Microorganisms capable of metabolizing complex and xenobiotic organics and toxins, *e.g.*, *Acinetobacter* spp., *Burkholderia* spp., and *Phenylobacterium* spp.,

were assigned to group four. In group five, microorganisms capable of directly affecting Au biogeochemical cycling were identified. These include putative Au mobilizers, *e.g*., the sulfur-oxidizing bacterium *Diaphorobacter sp.* and *Methylobacterium* spp. Other species, such as *Pseudomonas* spp., *C. metallidurans, D. acidovorans, Stenotrophomonas* sp., and *Achromobacter* spp., have the ability to actively detoxify Au-complexes *via* biomineralization (Rea, Zammit and Reith 2016; Reith et al. 2018). Dispersal cells are formed by species that comprise group six, including *Lysobacter* spp. and *Duganella* spp.

Studies by Brugger et al. (2013) and Etschmann et al. (2016) have demonstrated a biogeochemical link between bacterial community composition from Au and Pt particles and the mobility of these metals in natural environments. However, a study assessing biofilm composition and development in relation to Au particle transformation has not yet been conducted and is the aim of this study. In doing so, this study uses Au particles to: (i) characterize secondary Au structures, (ii) evaluate the degree of Au particle transformation, (iii) determine the presence of biofilms, and (iv) analyze the phylogenetic composition and functional capabilities of biofilm communities.

2. MATERIALS AND METHODS

2.1. Description of field sites and sampling

Primary Au deposits are widespread across the United Kingdom (UK) and Au mining activity predates Roman arrival on the British Isles. Peak exploitation of Au deposits occurred between *ca.* 1860 and 1910, where >3.5 t of Au was recovered (Colman 2010). Most primary deposits in the UK are hosted in Proterozoic to Permian aged rocks. Of the primary Au deposits, orogenic deposit-types are most abundant; however, porphyry, epithermal, and unconformity-related redox deposit-types also exist (Gunn and Styles 2002). Physical weathering of these primary deposits results in the formation of secondary deposits such as eluvial and alluvial placer deposits containing primary Au particles that have been

transformed by a range of physical and (bio)geochemical processes (Fairbrother et al. 2012; Reith, Stewart and Wakelin 2012; Reith et al. 2013).

For this study, Au particles were collected from eight placer sites that were proximal, *i.e.*, within 300 m, to primary deposits located in southern England and Scotland (Fig. S1; Colman 2010). Samples of Au particles were obtained using a field sterile method described by Reith et al. (2010) to minimize contamination and to preserve the integrity of the biofilm communities. See Table S1 for detailed descriptions of site location, deposit-style and environmental settings.

2.2. Electron microscopy and microanalyses

Samples were washed with sterile saline solution (0.9 wt. % NaCl) and placed in fixative (4 wt. % paraformaldehyde, 1.25 wt. % glutaraldehyde in PBS, 4 wt. % sucrose, pH 7.2) for at least 24 hours. These fixed Au particles were dehydrated using series of ethanol washes (70, 90 and 2 x 100 vol. %; 10 min each concentration), placed in 100 wt. % hexamethyldisilazane and air dried in the method described by Fratesi et al. (2004). The samples were carbon-coated and analyzed using a FEI Quanta™ 450 Field Emission Gun Scanning Electron Microscope (FEG-SEM) with Energy Dispersive Spectrometers (EDS) (FEI, Netherlands). Images were taken in Secondary Electron (SE) and Backscattered Electron (BSE) modes using 5 kV and 20 kV, respectively. Selected Au particles were further analyzed using an FEI Helios NanoLab DualBeam Focus Ion Beam (FIB)-SEM (FEI, Netherlands). Surface features were characterized in SE and BSE mode using 2 and 20 kV, respectively. An ion beam of 20 kV and 9.7 pA was used for FIB-milling micrometer-size cross-sections made on the surface of Au particles. The FIB-SEM is equipped with energy dispersive X-ray spectroscopy (EDXA) that was used to collect spectra/maps across

the particles surfaces and FIB-milled sections. Elements that were mapped included Au, Ag, Fe, C, N, O, Si, Ti, Al, Ga, Mg, Na, K and Pt.

A total of 28 Au particles were embedded in epoxy resin and polished with 1 µm-size diamond paste to make cross-sections of entire Au particles. These polished cross-sections were analyzed using a Cameca™ SXFive Electron Microprobe (EPMA), operating at 20 kV and 200 nA, (Cameca, France) was equipped with five wavelength dispersive X-Ray detectors. The Au particles were analyzed for the following elements with detection limits given in wt. %: Au (0.24 wt. %), Ag (0.09 wt. %), S (0.025 wt. %), Fe (0.06 wt. %) and Cu (0.11 wt. %). These elements were calibrated using chalcopyrite (Cu, Fe and S), telluride (Ag) and pure Au metal standards purchased from Astimex or P&H. The EPMA software produces a full quantitative pixel by pixel calculation by using the Mean Atomic Number background correction (Donovan and Tingle 1996) in CalcImage, and false colorization and formatting in Surfer10™ to produce net intensity, detection limit and totals image maps.

To estimate the extent of Au particle transformation, EMPA maps were analyzed using Image J v.1.50g (National Institutes of Health, USA; Abràmoff, Magalhães and Ram 2004; Rasband 2012). This analysis was performed by converting Au-Ag EMPA maps into binary images and calculating pixel by pixel ratios, *i.e*., a ratio of transformed secondary Au to untransformed primary Au. This transformation factor (TF) was calculated for each Au particle and the following TF stages were assigned: A (≤ 10%), B (11–20%), C (21–30%), D (31–40%). These four TF stages were used as a basis for the statistical analyses described below.

2.3. Biomolecular and statistical analyses

Additional Au particles were collected and used for microanalyses and DNA analyses. Biofilm communities from Au particles were assessed using nested 16S rRNA polymerase chain reaction (PCR) combined with next generation sequencing (NGS) using the Illumina MiSEQ platform – TruSeq SBS v.3 600 cycle using 300 bp paired end sequencing (Reith et al. 2010; Bissett et al. 2016). The universal primers 27F (Lane 1991) and 1492R (Osborn, Moore and Timmis 2000) were used for initial PCR amplification of 16s rRNA genes (Reith et al. 2010). Further amplification using primers 27F and 519R (Lane et al. 1985; Lane 1991) and sequencing at the Australian Genome Research Facility (AGRF, Melbourne, Australia) was performed. DNA amplifications were performed in an Applied Biosystems Veriti™ Thermal Cycler (Applied Biosystems, California, USA). Amplicons were checked in 1.5% agarose gel with Gel Red (Biotium Inc., Hayward, CA, USA) 1:10,000 (v/v) and run at a constant voltage of 80 V for 1 h. Procedures for sequencing, open OTU picking and assignment are detailed in Bissett et al. (2016). Briefly, sequence read quality was visually assessed using FastQC (Andrews 2010). Sequences were trimmed to remove poor quality bases and merged using FLASH (Magoč and Salzberg, 2011). Sequences <400 bp or containing N or homopolymer runs of >8 bp were removed (MOTHUR v1.34.1; Schloss et al. 2009). Remaining sequences were submitted to open reference (OTU) picking at 97 % sequence similarity using UPARSE (Edgar 2013) and OTU abundance tables constructed by mapping all reads to the OTUs (usearch_global, 97 %). Sequences were deposited in GenBank with accession numbers MG373505-MG373528.

Multivariate statistical analyses were conducted using the PRIMER-6 software package with the PERMANOVA+ add-on (Clarke and Warwick 2001; Anderson, Gorley and Clarke 2008). Similarity matrices were established on fourth root transformed abundance data using the Bray-Curtis method (Bray and Curtis 1957). PERMANOVA analyses were conducted using partial sums of squares on 9999 permutations of residuals under a full model. Non-metrical multidimensional scaling (nMDS) and canonical analysis of principal

coordinates (CAP) were used to assess the community differences between progressively transformed Au particles. Vector overlays, based on Pearson correlations, were used to explore relationships between significant individual variables and taxa and the ordination axes. CAP analyses were conducted based on the respective resemblance matrices with significance of test effects determined against null distributions based on 9999 permutations (random allocations) of samples. SIMPER analysis was used to assess groups/phyla that discriminate between transformation stages. Maximum-likelihood (1000 bootstrap replicates) phylogenetic trees were constructed using GENEIOUS 11.0.2 (Biomatters Ltd., New Zealand). Functional assignment of OTUs to the six groups representing the different stages of biofilm development was conducted based on the classification developed by Rea et al. (2016), wherein groupings are based on the dominant functional abilities of each organism.

3. RESULTS

3.1. Morphology and composition of Au particles and particle surfaces

All Au particles ranged from 0.1 to 2 mm in size (Fig. S1; Table S1) and demonstrated a range of morphologies including angular, hackly, slightly rounded, and wiry shapes. Some sites contained Au particles that were elongated and refolded (Fig. S1D–H; Table S1). The surface of Au particles demonstrated a range of articulation, *e.g.*, rounded to sub-rounded, scratched and abraded surfaces, which can be attributed to physical processes of Au particles during transport from the primary source (Townley et al. 2003).

The surface of Au particles contained crevices (Fig. 1A) that contained polymorphic layers primarily composed of bacterial cells (Fig. 1B), EPS (Fig. 1C) and Fe-oxides, clays, silicate minerals inferred from EDS analysis (Fig. 1D). These polymorphic layers were more than 20 µm thick. In some regions, EPS appeared to be in direct contact with Au particle

surfaces (Fig. 1E). Individual prokaryotic cells appeared attached directly on the Au particle surface (Fig. 1F).

Evidence of biogeochemical transformations were common on all Au particles. This included features of irregular pitting on the Au particle surface and is attributed to Ag and Au dissolution (Fig. 2). These dissolution features were often in close proximity to secondary Au structures (Fig. 3A) as well as appearing embedded within Fe-oxides, clays, silicate minerals (Fig. 3B). Gold nanoparticles occurred as triangular, hexagonal and polygonal shapes (Fig. 3C). Aggregates of these Au nanoparticles and other secondary Au structures, *i.e.*, bacteriform Au and crystals, appeared to form bridging-like structures that covered the Au particle surface (Fig. 3D). Regions of polymorphic layers contained abundant EPS and an abundance of aggregated Au nanoparticles as well as micrometer-size Au structures (Fig. 4A–D). These aggregates often formed sheet-like structures of secondary Au that covered the Au particle surface. These layers were composed of >99 wt. % Au, compared to the underlying primary Au-Ag alloys, which contain up to 30 wt. % Ag (Fig. 4E, F).

Microprobe analysis confirmed that Au particles contained Au-Ag alloy in the core and Au-rich rim on the outer edge of the Au particle. These rims were up to 100 µm in thickness and shows progressive transformation of a typical Au-Ag alloy (Fig. 5A) to Au-rich rim (99.9 wt. % Au) (Fig. 5). The extent of particle transformation that were assigned based on the binary image of the Au-Ag maps generally shows that Au particles from the same site displayed similar transformation stages. The assigned transformation for Au-particles from sampling location Ghanmain (GH), Ochill Hills (OHB/OHS), Mannock (MW) and Brownstone (BS) is TF group A, Snarwater (SN) is group B, Whympston (WY) and Glengonnar (GDO) is group C and Snails Cleuch Lammermuir Hills (LMH) is group D (Table S2).

3.2. Assessment of biofilm communities

The 16S rRNA gene was amplified to assess the composition of biofilm communities on the particles. More than 90% of Au particles were positive for target amplicons with greater than 2.3 million reads from 55 selected Au particles. Across all sites, 1610 different OTUs were detected, ranging from 85 at GH to 486 at LMH (Table S3). At the phylum level, Proteobacteria comprised the highest number of detected OTUs (39.9%; Fig. 6A) and more than half of the total sequence reads (59.3%; Fig. 6B). Within the Proteobacteria, β-Proteobacteria dominated with 270 OTUs and 29.6% of total reads. δ-Proteobacteria was numerous with 166 detected OTUs, which made up 11.0% of total reads; α- and γ-Proteobacteria with 124 and 104 detected OTUs, respectively, made up 3.2% and 7.6% of total reads and ε- Proteobacteria with 11 OTUs, made up of 7.6% of total reads (Fig. 6; Table S3). The phyla Acidobacteria and Bacteroidetes were also abundant with 246 and 255 OTUs, making up 7.9% and 9.9% of total reads, respectively. Other detected phyla included: Planctomycetes (7.9 and 3.0%, OTUs and reads), Verrucomicrobia (7.9 and 1.1%,) and 1.0–6.8% for Bacilli, Clostridia, Cyanobacteria, Nitrospirae and 22 other rarer phyla (Table S3). Across all sites, six OTUs classified from three genera were detected on all particles; these were *Rhodoferax* spp., *Geobacter* spp. and *Pseudomonas* spp., respectively (Fig. 7A). Eighteen OTUs were detected on 70% of the site (Fig. 7A; Table S4). CAP analyses of *Rhodoferax* spp. *and Geobacter* spp., (Fig. 7B, C) in relation to transformation factors shows no significant grouping for *Rhodoferax* with transformation grade; with *Geobacter* spp. forming distinct clusters with transformation grade. Non-metric MDS ordination of community assemblages showed a wide variety of communities associated with grains from TF A sites, with more distinct clustering in TF C and D. PERMANOVA showed that community composition varied with site ($\sqrt{CV} = 33.77$; $P < 0.001$) and degree of transformation ($\sqrt{CV} = 21.92$; $P < 0.001$). CAP analyses of community data illustrates the significant links of bacterial communities from Au particles with the transformation stages and biofilm group classification ($P < 0.001$; Fig. 8). Based on their assigned biofilm groups, organism known as

surface colonizer under group one is *Terribacillus* sp., which also has highest reads on Au particles from UK. OTUs assigned to group two can produce abundant EPS such as *Aeromonas* sp. and *Arcobacter* sp. In group three are organisms known to take part in nutrient cycling including *Geothrix* sp., *Nitrospira* sp., and *Sulfuricurvum* sp. Organisms detected that can perform metabolic turnover of complex and xenobiotic organics and toxins under group 4 included *Flavobacterium* sp., *Paucibacter* sp., and *Polaromonas* sp. Group five contains organisms that are involved in heavy metal cycling and metal detoxification, such as *Geobacter* spp., *Leptothrix* sp., *Pseudomonas* spp., *Rhodoferax* spp. Organisms forming dispersal cells are included in group six, *e.g*., *Lysobacter* sp. (Fig. 9).

4. DISCUSSION

The morphology and extent of transformation of Au particles in this study were similar to those observed on Au particles from different climatic environments from Australia, New Zealand, Finland and South America (Reith and McPhail 2006, 2007; Falconer and Craw 2009; Reith et al. 2010, 2018; Reith, Stewart and Wakelin 2012; Shuster et al. 2015, 2017; Craw and Lilly 2016). These features are the result of mechanical reshaping due to physical factors combined with bio(geo)chemical Au/Ag dissolution and re-precipitation processes occurring under surficial environmental conditions. The presence of polymorphic layers, composed of microbial cells, EPS, clays and other minerals, *e.g*., Fe-oxides and sulfides, fosters the sorption, embedding and accumulation of Au nano- and micro-particles (Fig. 3B, C; Reith et al. 2010; Reith and Cornelis 2017). Aggregations and spongy-form overgrowths of Au nano- and micro-particles (Fig. 3D, 4), with their intricate shapes, have likely formed *in situ*, as they would not survive transport as reported in studies from New Zealand (Reith, Stewart and Wakelin 2012, 2018; Craw, Hesson and Kerr 2017). The presence of EPS, particularly around the spheroidal and chained Au precipitates (Fig 4A–C), supports the suggestion of a strong bio-organic influence on secondary Au formation,

accumulation and aggregation at the UK sites. Subsequently, nano- and micro-crystalline layers are formed, which are indicative of a link of active dissolution/re-precipitation processes and physical re-crystallization reactions on grain boundaries (Falconer and Craw 2009). Striated textures within concavities (Fig 4A) are possibly relics of Au-Ag dissolution associated with active sulfur cycling (Shuster et al. 2017b). Overall particle shapes, including rounding, folding and scratches are often the results of physical transport in a sedimentary placer environment.

Biofilms are a ubiquitous part of bacterial life and documented on many natural, biological and anthropogenic surfaces (Hall-Stoodley et al. 2004), including placer Au particles from Australia, New Zealand and South America, where commonly 10 to 30 OTUs have been reported to comprise the multispecies biofilms covering the Au particles (Reith et al. 2006, 2010; Shuster et al. 2015; Rea, Zammit and Reith 2016). Far higher numbers of OTUs ranging from 85 at GH to 486 at LMH on each site were detected on Au particles in this study. The difference in number of detected OTUs is likely a result of improved resolution of NGS compared to the older PCR-DGGE-Sanger-sequencing technique used in earlier studies. This is supported by the results of another study using NGS with Au particles from 10 adjacent sites from Finland where 519 different OTUs were detected on placer Au (Reith et al. 2018). The higher number of OTUs detected on UK *vs*. Finnish particles may be linked to the closer spatial relationship of the Finnish sampling sites, which were located within a radius of 50 km, compared to the more widely dispersed UK sites. However, they may also be linked to the presence of extracellular DNA (eDNA) associated with the abundant clay-organic material on the surface of UK Au particles. eDNA can represent a relevant fraction of total DNA, and thus a significant portion of the entire soil metagenome (Nielsen and Matz 2006; Carini et al. 2017). Particularly rich in eDNA are clay- and organic matter-rich materials from semi-aquatic environments (Ogram et al. 1988; Cai et al. 2006; Pietramellara et al. 2009), such as the polymorphic layers of grains collected from active fluvial placers in the UK. The polymorphic layers may serve as eDNA-sinks and thereby

provide a record of organisms associated with Au particles throughout their transformation history, given that biofilms are continuously evolving. Indeed, throughout its development different organisms with diverse metabolic capabilities are recruited to multispecies biofilms, so the biofilm community can divide the functional traits amongst various groups of organisms (Alvarez et al. 1998; Cai, Huang and Zhang 2006; Harrison, Ceri and Turner 2007).

Studies of multispecies biofilms have shown that exposure to toxic heavy metals can negatively or positively affect the functional relationships within biofilm communities (Koechler et al. 2015). For example, multispecies biofilms grown from Canadian oil sands were highly resistant to toxic heavy metals, induced biomineralization of metals, and compositionally changed little after exposure to heavy metals compared to unstressed controls (Golby et al. 2014). This suggests that resistance to metals in biofilms is induced in the short term through activation of resistance mechanisms within the existing biofilm species and not by changes to their species composition. Studies of placer Au particles from Australia and Finland have shown that depending on the environmental conditions, transformation stages similar to those observed at UK samples can be achieved within decades to ten millennia of biogeochemical transformation under Earth surface conditions (Shuster et al. 2017a; Reith et al. 2018). Within these timeframes, which also may apply to highly transformed particles collected in the UK, changes to community compositions appear to occur. This is confirmed by the results of another Australian study, which showed that in soils formed from Aeolian sediments that had been transported less than 10 000 years ago to a position overlying a polymetallic deposit, microbial communities showed strong species-level differences compared to adjacent background soils (Reith et al. 2015).

The extensive library of detected organisms from present and/or past iterations of biofilms on the particles from the UK allows a more in-depth study of the link between progressive Au particle transformation, and the biofilm composition and functional capabilities, compared to earlier studies, where these links were implied based on the

presence of multi-metal resistant bacteria (Reith et al. 2006, 2010). Canonical analysis of principal coordinates has shown a significant link of community composition to the grade of secondary Au particle transformation at the UK sites (Fig. 8B). Gold particles that were TF stage A, *i.e*., ≤ 10% transformed, are likely at an early stage of recruitment which require microbial communities capable of establishing a biofilm that are increasingly resilient to metal toxicity from transforming particles, especially Au and Ag toxicity. Both metals are mobilized from the primary Au-Ag alloys of the particle core, but whereas Au is re-precipitated largely *via* biomineralization, Ag is lost to the environment, where it can form secondary Ag-containing minerals (Shuster et al. 2017b). To establish a biofilm, organisms from the immediate environment of the Au particle are recruited leading to communities that initially differ strongly between different sites, as shown in this study (Fig. 8A). Organisms linked to this stage of transformation are *Arcobacter* sp., and *Sulfurospirillum* sp. of group two and three, as well as *Sulfuritalea* spp., *Leptothrix* sp., and *Dechloromonas* spp., of group five respectively (Fig. 8C). *Arcobacter* sp., a Gram-negative ε- Proteobacteria, can set the framework of the biofilm community by hyperproduction of EPS to form polymeric bridges and promote flocculation (Mueller 2015). Polysaccharide-mediated aggregation of EPS and polymers, can increase water retention, water being essential to the growing biofilm (Hall-Stoodley et al. 2004). *Sulfurospirillum* sp., contribute to the S cycle and can produce H_2S, as ligand that can leach Au by formation of Au-complexes (Shuster and Southam 2015). Organisms strongly involved in S, P and N cycling are often less resistant to metal stress since microbial energy is primarily used for various enzymatic activities (Azarbad et al. 2016). Thus, we also expected recruitment of biofilm members that can reduce the stress occurring at an early transformation stage of Au particles. These can be achieved by members of the biofilm group five, *Leptothrix* sp., an Fe-oxidizing organism and *Dechloromonas* spp*.,* a facultative anaerobe that uses a heavy metal efflux pump, which can strengthen the biofilm by horizontal gene transfer of inherent genes to other compatible members of the biofilm community (Hall-Stoodley et al. 2004; Harrison, Ceri and Turner 2007).

A more metal-resistant biofilm community evolves as the degree of Au transformation increases, and as a result biofilm communities become increasingly similar between sites (Fig. 8). This is likely due to an increase in metal toxicity from elevated concentration of mobilized Au and Ag and other pathfinders mobilized from the transforming primary Au particles and Au bearing minerals. Organisms belonging to the metallophilic group five linked to 21–30% transformation that will have the most profound effect on metal detoxification and Au-mobility are *Pseudomonas* spp., *Fusibacter* spp., *Acinetobacter* spp., *Rubrivivax* sp., as well as the exoelectrogens *Rhodoferax* spp., and *Geobacter* spp. *Pseudomonas* spp. are Gram-negative, ubiquitous, often heavy metal resistant γ-Proteobacteria, which have now been detected on Au-particles from the UK (this study), as well as Brazil and Australia, where they have been shown to dominate communities on particles from some sites (Rea, Zammit and Reith 2016). *Pseudomonas* spp., *e.g*., *P. aeruginosa*, *P. putida* and *P. plecoglossicida,* are known for their ability to form biofilms and be able to resist up to 600 times higher heavy metal concentrations compared to planktonic cells (Teitzel and Parsek 2003; Meliani and Bensoltane 2016). Gold accumulation in exopolymeric substances played a role in the detoxification of Au(III)-chloride by *P. aeruginosa*, which displayed a four times higher viability when grown as a biofilm compared to free planktonic cells when subjected to 0.1 mM Au(III)-chloride (Karthikeyan and Beveridge 2002). *Pseudomonas* spp. can produce metabolic products or chelating compounds to solubilize metals from clays and organic matter minerals (Mueller 2015).

Also detected on Au particles from all sites in the UK were members of the putative exoelectrogenic genera *Geobacter* spp., and *Rhodoferax* spp., which can act as initial colonizers on metallic or solid substrates due to their innate affinity to metals (Dopson, Ni and Sleutels 2016). *Geobacter* spp., an anaerobic δ-Proteobacteria, can pass electrons from organic compounds and clays to Fe-oxides and metal surfaces using nanowires to release and harvest electrons (Richter et al. 2008). *Rhodoferax* spp., purple non-sulfur phototrophic β-Proteobacteria, can form persistent biofilm layers on surfaces and oxidize glucose to

produce electricity (Chaudhuri and Lovley 2003). Both exoelectrogenic genera, can use suitable mineral inclusions, biofilm biomass, and most likely Au surfaces to precipitate Au and perform electron “dumping” on the surface for use by other microorganisms (Lloyd et al. 2003; Richter et al. 2008). The process of electron “dumping” is mediated by cytochromes, Fe/S-proteins, by direct electron transfer *via* nanowires or indirect transfer using soluble redox shuttles such as humic acid or inorganic S and H_2S (Reguera et al. 2005; Liu et al. 2014). Microbial-assisted production of electrons directly from organic matter and solid mineral surfaces is beneficial for the microorganisms to extract energy, remove recalcitrant compounds, and drive their microbial metabolism and possibly drive the metabolic activity of the whole biofilm community (Dopson, Ni and Sleutels 2016; Nevin et al. 2011). Electric signals produced by exoelectrogens mimics the quorum sensing molecule to communicate and attract other organisms (Humphries et al. 2017). The projected electrical signals attract distant cells of similar or an entirely unrelated species, to recruit into the growing biofilm community (Prindle et al. 2015; Humphries et al. 2017; Liu et al. 2017). Apparently, multi-layer biofilms can use this ‘electric potential’ to communicate more effectively; where inner cells can send electric signals to outer cells of the biofilm more efficiently than using quorum sensing molecules (Liu et al. 2017). This means that recruitment of several other microorganisms that form compounds which reacts with Au particles can be mediated by these exoelectrogens. For instance, recruitment of SRBs and SOBs, e.g. *Sulfuricurvum* sp., and *Fusibacter* spp., both linked to TF stage C, can produce derivatives of sulfur that contribute to Au mobility, as well as other metallophiles capable of Au detoxification *via* biomineralization. Copper-resistant organisms detected on Au particles from the UK, *e.g*., the facultative photoheterotrophic β-Proteobacteria *Rubrivivax* spp., may synergistically detoxify Cu-ions and Au-complexes to protect the general population present on the biofilm community (Azzouzi et al. 2013). Resistance to one specific metal may provide cross resistance or co-tolerance to other metals; the co-tolerance increases the resistance to one stressor as a result of an earlier exposure to a similar stressor, as recently shown for *C. metallidurans* CH34*,* an aurophillic aerobic β-Proteobacterium detected on Au particles from

Australia and Brazil. *Cupriavidus metallidurans* can reduce toxic Au(I/III)-complexes in the periplasm via synergistic co-utilization and regulation of Cu/Au resistance determinants by the metal chaperone CupC and the periplasmic Cu-oxidase CopA (Wiesemann et al. 2013, 2017; Zammit et al. 2016; Bütof et al. 2018)**.**

However, biofilm mediated Au transformation may not occur effectively without the 'helpers' in the biofilm community other than those under groups two, three and four. These organisms keep the biofilm community functioning and are protected from metal toxicity through the activity of the group five organisms, which can detoxify heavy metals. In UK samples these organisms include putative primary colonizers (group one), like the Gram-positive bacterium *Terribacillus* sp. Gram-positive bacteria can easily overcome the negatively charged surface of Au-particles and associated clay-like minerals (Paget, Monrozier and Simonet 1992; Rea, Zammit and Reith 2016). This is supported by the strong link of diverse organisms to Au particles that were > 20% transformed, which include biofilm group two *Aeromonas* sp., group three *Massilia* sp., and *Sulfuricurvum* sp., group four *Herminiimonas* sp.*,* and *Polaromonas* sp. Organisms that can produce and recycle biomass in the biofilm under group four includes *Herminiimonas* sp. and *Polaromonas* spp., also reported from a Finnish site, these are more resistant and resilient to environmental stressors because of functional redundancy. This means that the stress response is not focused in these organisms because other microorganisms previously recruited in the biofilm can share a similar function (Azarbad et al. 2016). When biofilms have reached the maximum carrying capacity, it requires the release of cells to decrease microbial load. The killing kinetics of microbial populations may be related to specific cell types that can withstand the action of metal toxicity such as those of persister cells that can form exponentially to mediate time-dependent tolerance to metal cations and oxyanions (Harrison, Ceri and Turner 2007). In addition, dead cells interspersed with live cells are chemically reactive biomasses that bioabsorb and drive metal precipitation or chelation, preventing the ions from interfering in sensitive metabolic processes (Hall-Stoodley et al.

2004). The formation of this dispersal and dead cells, to decrease microbial load and release particles, is regulated by group six organisms, such as *Lysobacter* sp., present on 70% of the Au-particles and also detected in Australian Au-particles. The dead and dispersal cells further increase mobility of Au and trace metals as they detach from the biofilm community.

5. CONCLUSIONS

In this study, we show that a highly diverse biofilm community with a wide-range of metabolic capabilities is present on Au particles from placer deposits in the United Kingdom. Furthermore, all particles were associated with a variety of secondary Au morphotypes likely resulting from the biomineralization of Au by resident taxa. These taxa may be able to reductively precipitate toxic mobile Au complexes as well as act as exoelectrogens which dump excess electrons on Au surfaces, whereas other members produce metabolic products, chelating compounds to solubilize metals and mobilize Au embedded in clay-like minerals. Others can exhibit co-tolerance by co-utilization and regulation of Cu-Au resistance, similar to the widely reported aurophilic Proteobacterium *C. metallidurans*. Overall, this is the first study to confirm a link between the composition and functional abilities of biofilm communities and the transformation stages of Au particles. Community assemblages recruited to the biofilm are initially different between sites and evolve to increasingly similar communities of metal-resistant members as the degree of Au transformation increases. This is likely due to increasing the load of toxic mobile Au and Ag experienced by communities during biogeochemical transformation.

Acknowledgements

We acknowledge the following institutions for their contributions: ARC-FT100150200 to F. Reith, Adelaide Microscopy (an Australian Microscopy and Microanalysis Research Facility),

the South Australian Museum. We are thankful to A. Basak, C.M. Zammit, J. Brugger, B. Etschmann, B. Wade, J. Zhao, K. Neubauer, G. Rinder, T. Reith, M. Maminta for their support. We are especially grateful to R.J. Chapman and M. Grimshaw for excellent field support and to the landowners at the sampling sites for site access.

References

Abràmoff MD, Magalhães PJ, Ram SJ. Image processing with ImageJ. *Biophotonics international* 2004;**11:**36-42.

Alvarez A, Khanna M, Toranzos G*, et al.* Amplification of DNA bound on clay minerals. *Mol Ecol* 1998;**7:**775-8.

Anderson M, Gorley RN, Clarke RK. (2008) *Permanova+ for Primer: Guide to Software and Statisticl Methods*: Primer-E Limited.

Andrews S. (2010) FastQC: a quality control tool for high throughput sequence data.

Azarbad H, van Gestel CA, Niklińska M*, et al.* Resilience of Soil Microbial Communities to Metals and Additional Stressors: DNA-Based Approaches for Assessing "Stress-on-Stress" Responses. *Int J Mol Sci* 2016;**17:**933.

Azzouzi A, Steunou AS, Durand A*, et al.* Coproporphyrin III excretion identifies the anaerobic coproporphyrinogen III oxidase HemN as a copper target in the Cu+-ATPase mutant copA− of Rubrivivax gelatinosus. *Mol Microbiol* 2013;**88:**339-51.

Bissett A, Fitzgerald A, Meintjes T*, et al.* Introducing BASE: the Biomes of Australian Soil Environments soil microbial diversity database. *GigaScience* 2016;**5:**1.

Bray JR, Curtis JT. An ordination of the upland forest communities of southern Wisconsin. *Ecol Monogr* 1957;**27:**325-49.

Brugger J, Etschmann B, Grosse C*, et al.* Can biological toxicity drive the contrasting behavior of platinum and gold in surface environments? *Chem Geol* 2013;**343:**99-110.

Bütof L, Wiesemann N, Herzberg M*, et al.* Synergistic gold–copper detoxification at the core of gold biomineralisation in Cupriavidus metallidurans. *Metallomics* 2018.

Cai P, Huang Q-Y, Zhang X-W. Interactions of DNA with clay minerals and soil colloidal particles and protection against degradation by DNase. *Environ Sci Technol* 2006;**40:**2971-6.

Cai P, Huang Q, Zhang X*, et al.* Adsorption of DNA on clay minerals and various colloidal particles from an Alfisol. *Soil Biology and Biochemistry* 2006;**38:**471-6.

Carini P, Marsden PJ, Leff JW*, et al.* Relic DNA is abundant in soil and obscures estimates of soil microbial diversity. *Nature microbiology* 2017;**2:**16242.

Chaudhuri SK, Lovley DR. Electricity generation by direct oxidation of glucose in mediatorless microbial fuel cells. *Nat Biotechnol* 2003;**21:**1229-32.

Checa SK, Espariz M, Audero MEP*, et al.* Bacterial sensing of and resistance to gold salts. *Mol Microbiol* 2007;**63:**1307-18.

Clarke K, Warwick R. A further biodiversity index applicable to species lists: variation in taxonomic distinctness. *Mar Ecol Prog Ser* 2001;**216:**265-78.

Colman T. Gold in Britain: past, present and future. *Mercian Geologist* 2010;**17:**173-80.

Craw D, Lilly K. Gold nugget morphology and geochemical environments of nugget formation, southern New Zealand. *Ore Geology Reviews* 2016;**79:**301-15.

Craw D, Hesson M, Kerr G. Morphological evolution of gold nuggets in proximal sedimentary environments, southern New Zealand. *Ore Geology Reviews* 2017;**80:**784-99.

Donovan JJ, Tingle TN. An improved mean atomic number background correction for quantitative microanalysis. *Microsc Microanal* 1996;**2:**1-7.

Dopson M, Ni G, Sleutels TH. Possibilities for extremophilic microorganisms in microbial electrochemical systems. *FEMS Microbiol Rev* 2016;**40:**164-81.

Edgar RC. UPARSE: highly accurate OTU sequences from microbial amplicon reads. *Nature methods* 2013;**10:**996-8.

Etschmann B, Brugger J, Fairbrother L*, et al.* Applying the Midas touch: Differing toxicity of mobile gold and platinum complexes drives biomineralization in the bacterium Cupriavidus metallidurans. *Chem Geol* 2016;**438:**103-11.

Fairbrother L, Brugger J, Shapter J*, et al.* Supergene gold transformation: Biogenic secondary and nano-particulate gold from aid Australia. *Chem Geol* 2012;**320:**17-31.

Fairbrother L, Shapter J, Brugger J*, et al.* Effect of the cyanide-producing bacterium Chromobacterium violaceum on ultraflat Au surfaces. *Chem Geol* 2009;**265:**313-20.

Falconer D, Craw D. Supergene gold mobility: a textural and geochemical study from gold placers in southern New Zealand. *Economic Geology Special Publication* 2009;**14:**77-93.

Fratesi SE, Lynch FL, Kirkland BL*, et al.* Effects of SEM preparation techniques on the appearance of bacteria and biofilms in the Carter Sandstone. *Journal of Sedimentary Research* 2004;**74:**858-67.

Golby S, Ceri H, Marques LL*, et al.* Mixed-species biofilms cultured from an oil sand tailings pond can biomineralize metals. *Microb Ecol* 2014;**68:**70-80.

Groen JC, Craig JR, Rimstidt JD. Gold-rich rim formation on electrum grains in placers. *The Canadian Mineralogist* 1990;**28:**207-8.

Gunn A, Styles M. Platinum-group element occurrences in Britain: magmatic, hydrothermal and supergene. *Applied Earth Science* 2002;**111:**2-14.

Hall-Stoodley L, Costerton JW, Stoodley P. Bacterial biofilms: from the natural environment to infectious diseases. *Nature Reviews Microbiology* 2004;**2:**95-108.

Harrison JJ, Ceri H, Turner RJ. Multimetal resistance and tolerance in microbial biofilms. *Nature Reviews Microbiology* 2007;**5:**928-38.

Humphries J, Xiong L, Liu J*, et al.* Species-independent attraction to biofilms through electrical signaling. *Cell* 2017;**168:**200-9. e12.

Johnston CW, Wyatt MA, Li X*, et al.* Gold biomineralization by a metallophore from a gold-associated microbe. *Nat Chem Biol* 2013;**9:**241-3.

Karthikeyan S, Beveridge T. Pseudomonas aeruginosa biofilms react with and precipitate toxic soluble gold. *Environ Microbiol* 2002;**4:**667-75.

Koechler S, Farasin J, Cleiss-Arnold J*, et al.* Toxic metal resistance in biofilms: diversity of microbial responses and their evolution. *Res Microbiol* 2015;**166:**764-73

Lane D. 16S/23S rRNA sequencing. *Nucleic acid techniques in bacterial systematics* 1991.

Lane DJ, Pace B, Olsen GJ*, et al.* Rapid determination of 16S ribosomal RNA sequences for phylogenetic analyses. *Proceedings of the National Academy of Sciences* 1985;**82:**6955-9.

Liu J, Chakraborty S, Hosseinzadeh P*, et al.* Metalloproteins containing cytochrome, iron–sulfur, or copper redox centers. *Chem Rev* 2014;**114:**4366-469.

Liu J, Martinez-Corral R, Prindle A*, et al.* Coupling between distant biofilms and emergence of nutrient time-sharing. *Science* 2017;**356:**638-42.

Lloyd JR, Leang C, Myerson ALH*, et al.* Biochemical and genetic characterization of PpcA, a periplasmic c-type cytochrome in Geobacter sulfurreducens. *Biochem J* 2003;**369:**153-61.

Magoč T, Salzberg SL. FLASH: fast length adjustment of short reads to improve genome assemblies. *Bioinformatics* 2011;**27:**2957-63.

McCready A, Parnell J, Castro L. Crystalline placer gold from the Rio Neuquen, Argentina: Implications for the gold budget in placer gold formation. *Economic Geology* 2003;**98:**623-33.

Meliani A, Bensoltane A. Biofilm-mediated heavy metals bioremediation in PGPR Pseudomonas. *J Bioremediat Biodegrad* 2016;**7:**370.

MetOffice (2015) *UK climate Summaries 2014 Annual*, accessed at http://www.metoffice.gov.uk/climate/uk/summaries/2014/annual.

Mueller B. Experimental interactions between clay minerals and bacteria: A review. *Pedosphere* 2015;**25:**799-810.

Nevin KP, Hensley SA, Franks AE*, et al.* Electrosynthesis of organic compounds from carbon dioxide is catalyzed by a diversity of acetogenic microorganisms. *Appl Environ Microbiol* 2011;**77:**2882-6.

Nielsen R, Matz M. Statistical approaches for DNA barcoding. *Syst Biol* 2006;**55:**162-9.

Nies DH. Microbial heavy-metal resistance. *Appl Microbiol Biotechnol* 1999;**51:**730-50.

Ogram A, Sayler GS, Gustin D*, et al.* DNA adsorption to soils and sediments. *Environ Sci Technol* 1988;**22:**982-4.

Osborn AM, Moore ER, Timmis KN. An evaluation of terminal- restriction fragment length polymorphism (T- RFLP) analysis for the study of microbial community structure and dynamics. *Environ Microbiol* 2000;**2:**39-50.

Paget E, Monrozier LJ, Simonet P. Adsorption of DNA on clay minerals: protection against DNaseI and influence on gene transfer. *FEMS Microbiol Lett* 1992;**97:**31-9.

Pietramellara G, Ascher J, Borgogni F*, et al.* Extracellular DNA in soil and sediment: fate and ecological relevance. *Biol Fertil Soils* 2009;**45:**219-35.

Prindle A, Liu J, Asally M*, et al.* Ion channels enable electrical communication in bacterial communities. *Nature* 2015;**527:**59-63.

Rasband W. ImageJ: Image processing and analysis in Java. *Astrophysics Source Code Library* 2012.

Rea MA, Zammit CM, Reith F. Bacterial biofilms on gold grains-Implications for geomicrobial transformations of gold. *FEMS Microbiol Ecol* 2016;fiw082.

Reguera G, McCarthy KD, Mehta T*, et al.* Extracellular electron transfer via microbial nanowires. *Nature* 2005;**435:**1098.

Reith F, Brugger J, Zammit CM*, et al.* Influence of geogenic factors on microbial communities in metallogenic Australian soils. *The ISME journal* 2012;**6:**2107-18.

Reith F, Brugger J, Zammit CM*, et al.* Geobiological cycling of gold: from fundamental process understanding to exploration solutions. *Minerals* 2013;**3:**367-94.

Reith F, Cornelis G. Effect of soil properties on gold-and platinum nanoparticle mobility. *Chem Geol* 2017;**466:**446-53.

Reith F, Etschmann B, Grosse C*, et al.* Mechanisms of gold biomineralization in the bacterium Cupriavidus metallidurans. *Proceedings of the National Academy of Sciences* 2009;**106:**17757-62.

Reith F, Fairbrother L, Nolze G*, et al.* Nanoparticle factories: Biofilms hold the key to gold dispersion and nugget formation. *Geology* 2010;**38:**843-6.

Reith F, Lengke MF, Falconer D*, et al.* The geomicrobiology of gold. *The ISME Journal* 2007;**1:**567-84.

Reith F, McPhail D. Effect of resident microbiota on the solubilization of gold in soil from the Tomakin Park Gold Mine, New South Wales, Australia. *Geochim Cosmochim Acta* 2006;**70:**1421-38.

Reith F, McPhail D. Mobility and microbially mediated mobilization of gold and arsenic in soils from two gold mines in semi-arid and tropical Australia. *Geochim Cosmochim Acta* 2007;**71:**1183-96.

Reith F, Rea MAD, Sawley P*, et al.* Biogeochemical cycling of gold: Transforming gold particles from arctic Finland. *Chem Geol* 2018.

Reith F, Rogers SL, McPhail D*, et al.* Biomineralization of gold: biofilms on bacterioform gold. *Science* 2006;**313:**233-6.

Reith F, Stewart L, Wakelin SA. Supergene gold transformation: Secondary and nano-particulate gold from southern New Zealand. *Chem Geol* 2012;**320:**32-45.

Reith F, Zammit CM, Pohrib R*, et al.* Geogenic factors as drivers of microbial community diversity in soils overlying polymetallic deposits. *Appl Environ Microbiol* 2015;**81:**7822-32.

Richter H, McCarthy K, Nevin KP*, et al.* Electricity generation by Geobacter sulfurreducens attached to gold electrodes. *Langmuir* 2008;**24:**4376-9.

Schloss PD, Westcott SL, Ryabin T*, et al.* Introducing mothur: open-source, platform-independent, community-supported software for describing and comparing microbial communities. *Appl Environ Microbiol* 2009;**75:**7537-41.

Shuster J, Southam G. The in-vitro “growth” of gold grains. *Geology* 2015;**43:**79-82.

Shuster J, Bolin T, MacLean LC*, et al.* The effect of iron-oxidising bacteria on the stability of gold (I) thiosulphate complex. *Chem Geol* 2014;**376:**52-60.

Shuster J, Johnston CW, Magarvey NA*, et al.* Structural and Chemical Characterization of Placer Gold Grains: Implications for Bacterial Contributions to Grain Formation. *Geomicrobiology Journal* 2015;**32:**158-69.

Shuster J, Reith F, Cornelis G*, et al.* Secondary gold structures: Relics of past biogeochemical transformations and implications for colloidal gold dispersion in subtropical environments. *Chem Geol* 2017;**450:**154-64

Shuster J, Reith F, Izawa MR*, et al.* Biogeochemical Cycling of Silver in Acidic, Weathering Environments. *Minerals* 2017;**7:**218.

Southam G, Lengke MF, Fairbrother L*, et al.* The biogeochemistry of gold. *Elements* 2009;**5:**303-7.

Stewart J, Kerr G, Prior D*, et al.* Low temperature recrystallisation of alluvial gold in paleoplacer deposits. *Ore Geology Reviews* 2017;**88:**43-56.

Ta C, Brugger J, Pring A*, et al.* Effect of manganese oxide minerals and complexes on gold mobilization and speciation. *Chem Geol* 2015;**407:**10-20.

Ta C, Reith F, Brugger Jl*, et al.* Analysis of gold (I/III)-complexes by HPLC-ICP-MS demonstrates gold (III) stability in surface waters. *Environ Sci Technol* 2014;**48:**5737-44.

Teitzel GM, Parsek MR. Heavy metal resistance of biofilm and planktonic Pseudomonas aeruginosa. *Appl Environ Microbiol* 2003;**69:**2313-20.

Townley BK, Hérail G, Maksaev V*, et al.* Gold grain morphology and composition as an exploration tool: application to gold exploration in covered areas. *Geochemistry: Exploration, Environment, Analysis* 2003;**3:**29-38.

Wakelin S, Anand RR, Macfarlane C*, et al.* Assessing microbiological surface expression over an overburden-covered VMS deposit. *Journal of Geochemical Exploration* 2012;**112:**262-71.

Wiesemann N, Bütof L, Herzberg M*, et al.* Synergistic toxicity of copper and gold compounds in Cupriavidus metallidurans. *Appl Environ Microbiol* 2017;AEM. 01679-17.

Wiesemann N, Mohr J, Grosse C*, et al.* Influence of copper resistance determinants on gold transformation by Cupriavidus metallidurans strain CH34. *J Bacteriol* 2013;**195:**2298-308.

Zammit CM, Weiland F, Brugger J*, et al.* Proteomic responses to gold (III)-toxicity in the bacterium Cupriavidus metallidurans CH34. *Metallomics* 2016;**8:**1204-16.

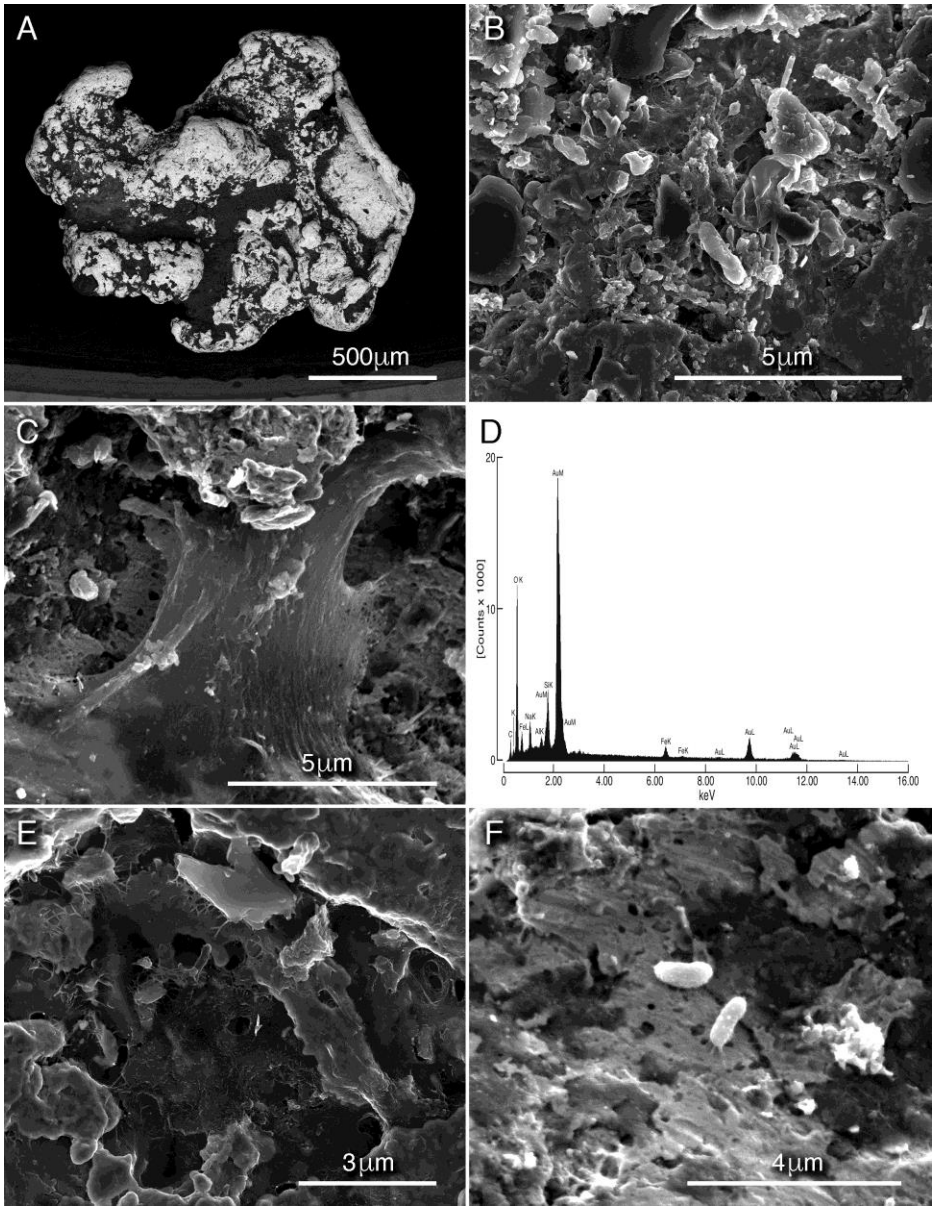

Figure 1 Electron micrographs of polymorphic layers on Au particle surfaces. (**A**) A Backscattered Electron (BSE) micrograph of a representative Au particle containing crevices filled with polymorphic layer. (**B–F**) Secondary Electron (SE) micrographs of remnant cells and EPS. **(D)** A representative spectrum of the elemental composition of Fe-oxide and silicate minerals. **(E, F)** SE micrograph of EPS and microbial cells in direct contact with the Au surface.

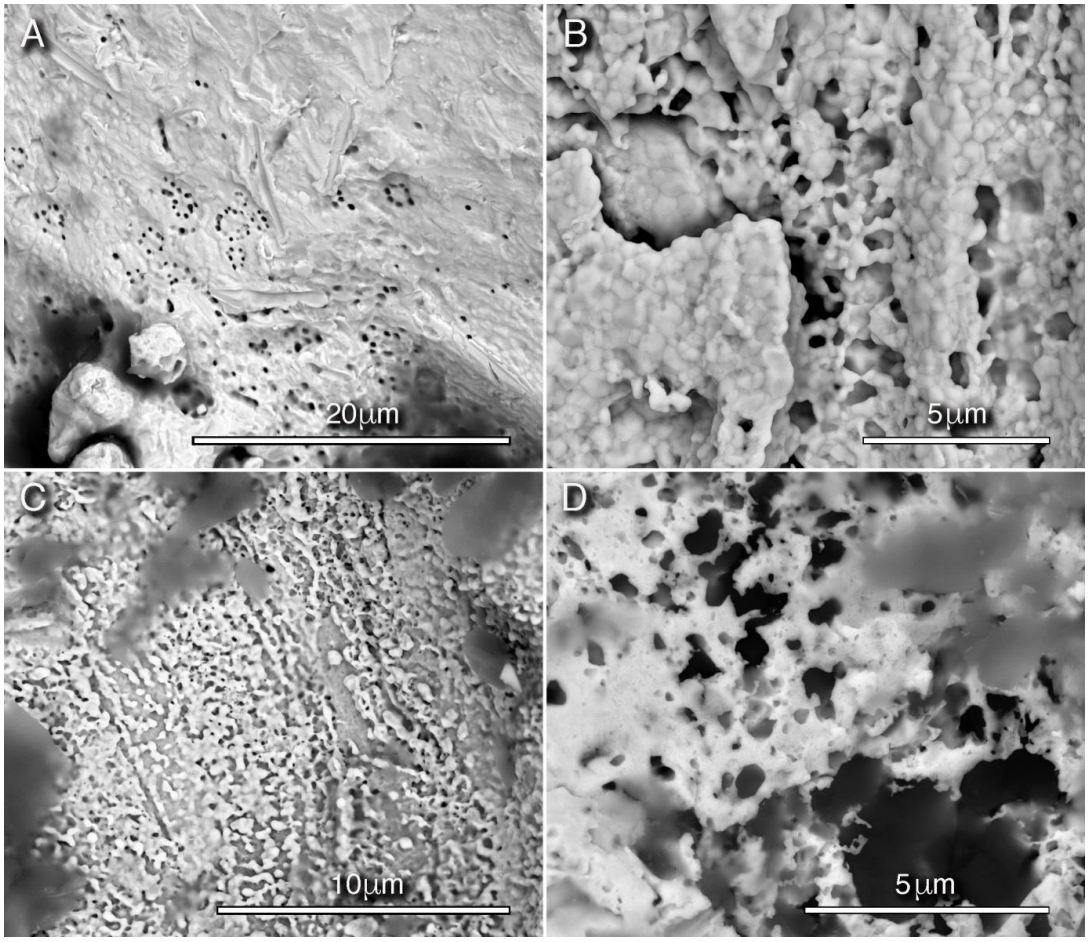

Figure 2 **(A)** A BSE micrograph of a Au particle surface. The pitted surface represents initial stages of Au/Ag dissolution. **(B-D)** BSE micrographs demonstrating progressive Au/Ag dissolution of Au particle surfaces leading to more irregular-size pitting and increased roughness of the Au particle surface; during this process Au and Ag are mobilized and released into the environment.

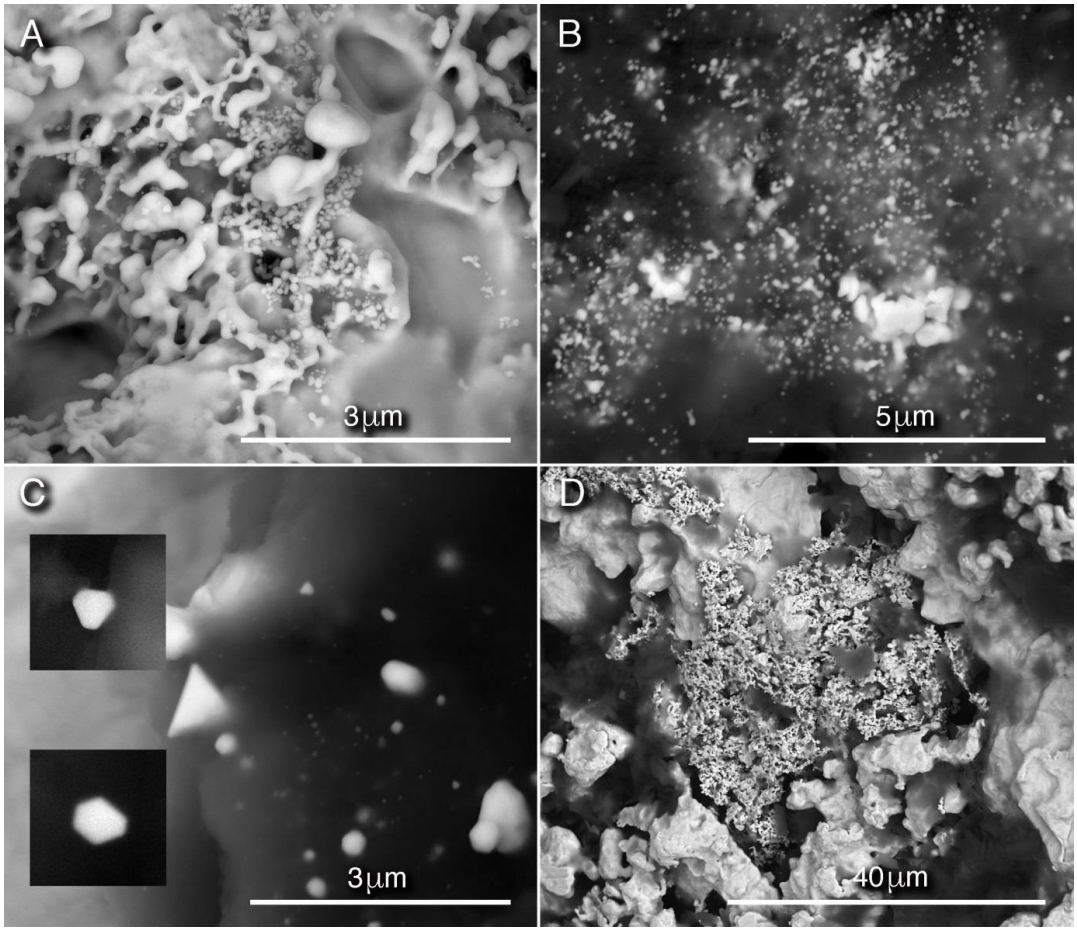

Figure 3 **(A, B)** BSE micrographs of Au nanoparticles in close association with Au/Ag dissolution features and embedded within clay minerals, respectively. **(C and inset)** BSE micrographs of Au nanoparticles associated with polymorphic layer. These Au nanoparticles appeared triangular, hexagonal and polygonal in shape. **(D)** A BSE micrograph of aggregated Au nanoparticles covering the surface of a primary Au particle.

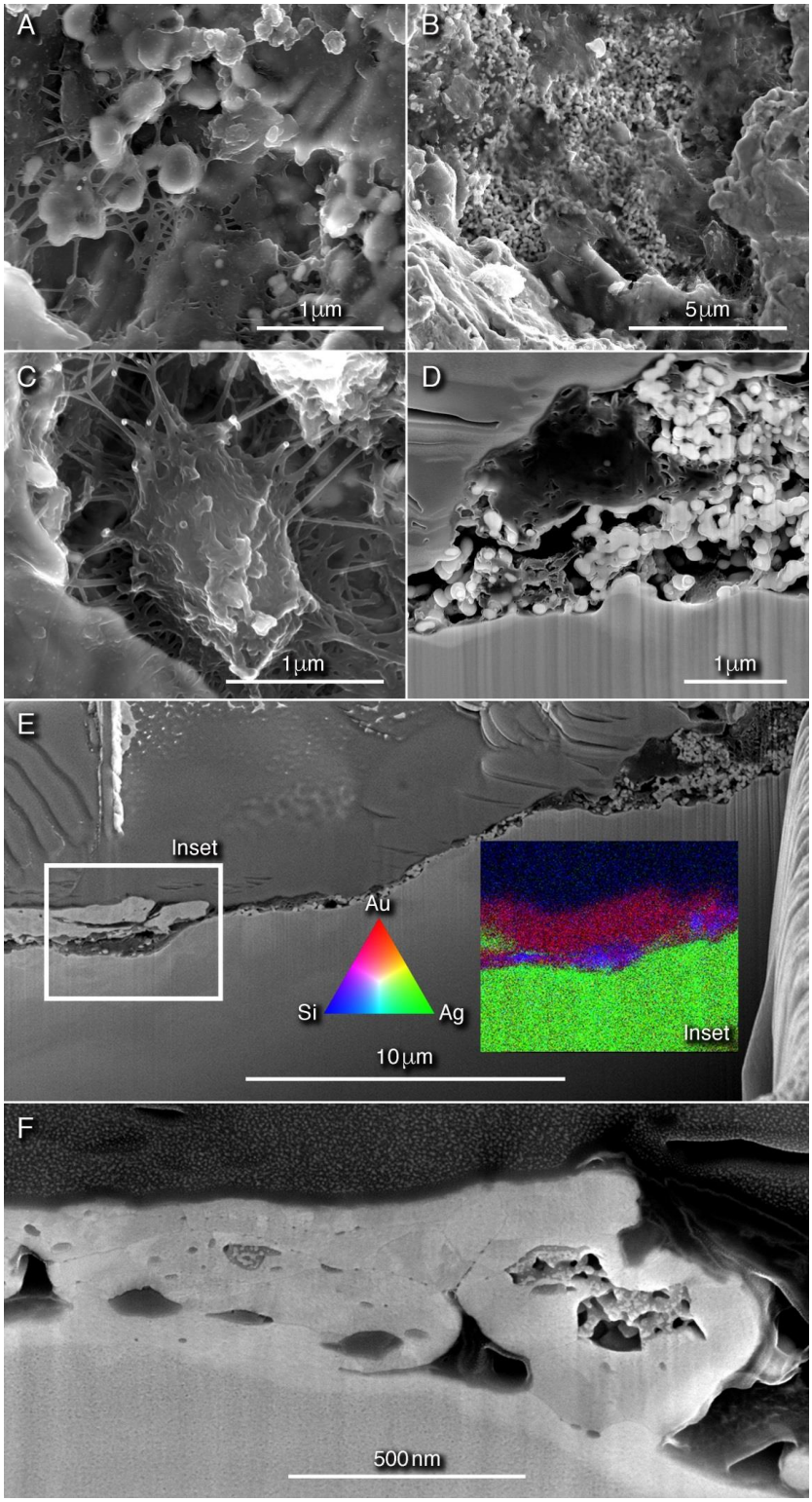

Figure 4 Micrographs of Au nano and μ-crystals (**A–C**) SE micrographs of Au nanoparticles and other secondary Au structure in close association with EPS. **(D)** An SE micrograph of a FIB-milled cross-section showing Au aggregates of Au nanoparticles covered by a polymorphic layer. **(E, F)** An SE

micrograph of a FIB-milled cross-section demonstrating a Au-enriched structure on the surface of a primary Au-Ag particle. This structure contains a nano-crystalline fabric.

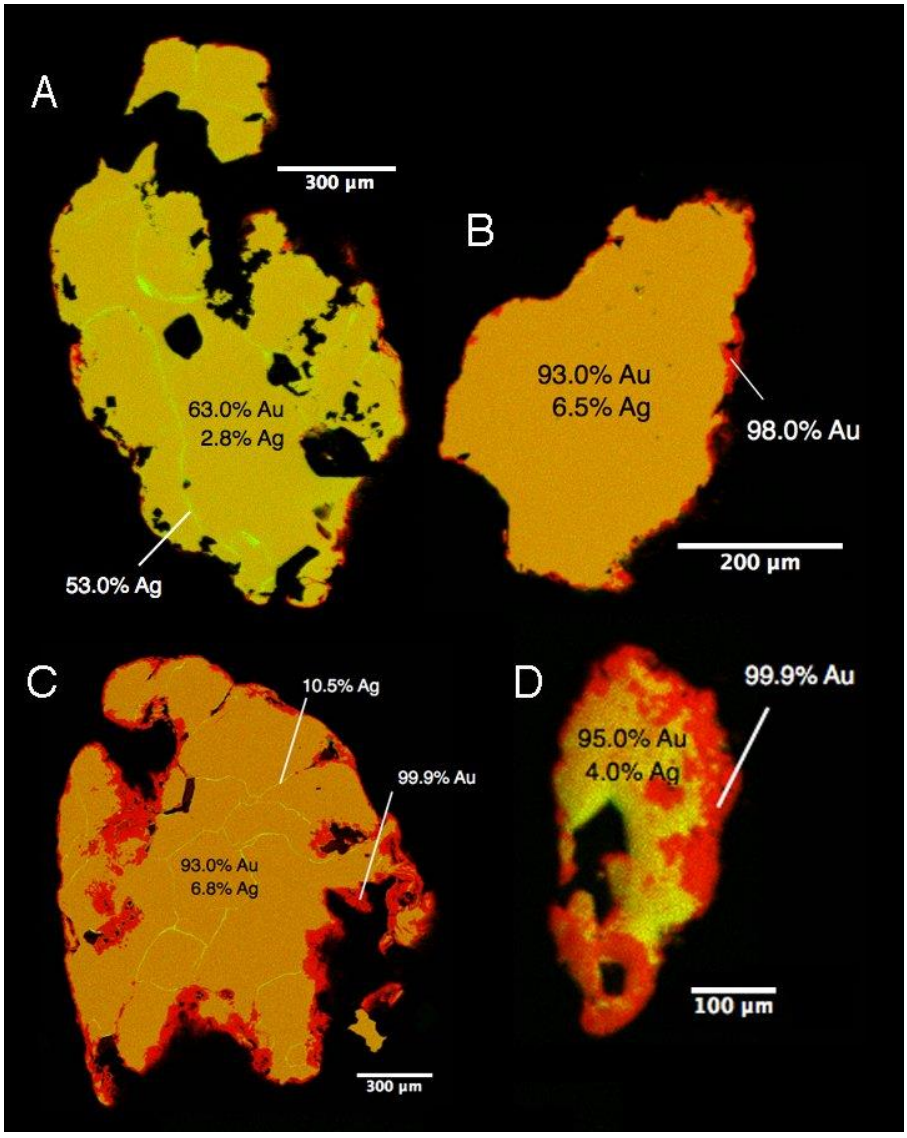

Figure 5 A series of representative EMPA maps of cross sections through Au particles demonstrating progressive transformation of Au particles. Au is represented by the color red while Ag represented by the color green. (**A**) A Au particle from TF stage A (i.e., ≤10 % transformation), **(B)** A Au particle from TF stage B (i.e., 11-20% transformation), **(C)** A Au particle from TF stage C (i.e., 21-

30% transformation) and **(D)** A Au particle from TF stage D (i.e., 31-40% transformation).

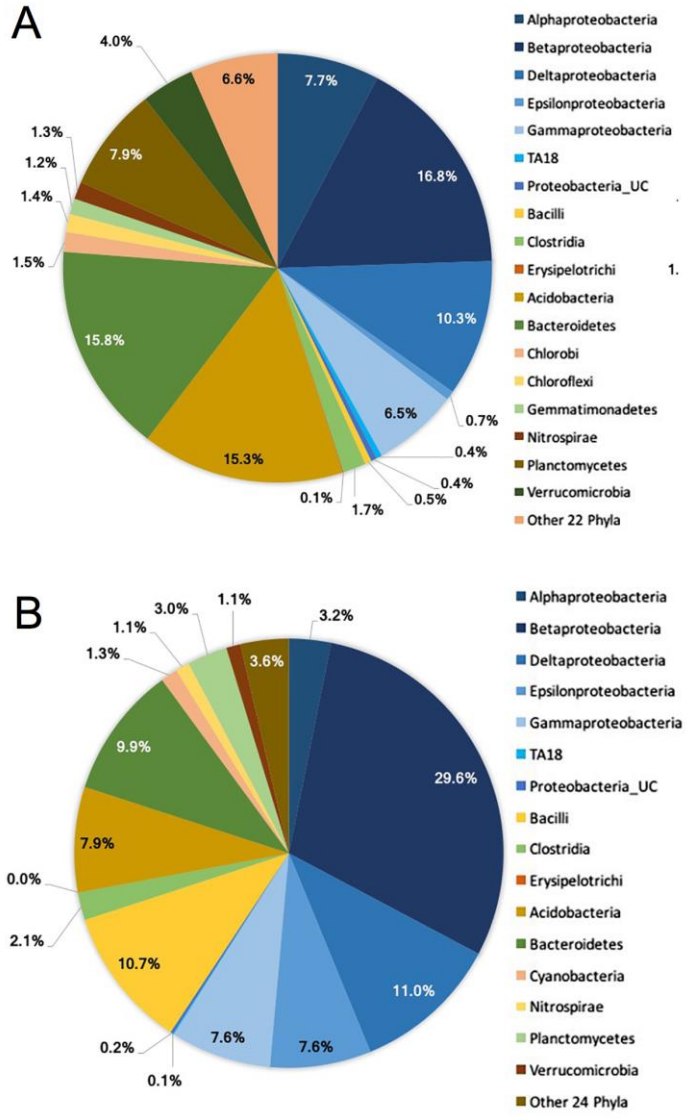

Figure 6 Composition of bacterial communities from Au particles. Distribution of dominant bacterial phyla/classes based on (**A**) number of OTUs (1610) and **(B)** OTU reads (>2.3 million). Note: classes are shown for Proteobacteria and Firmicutes.

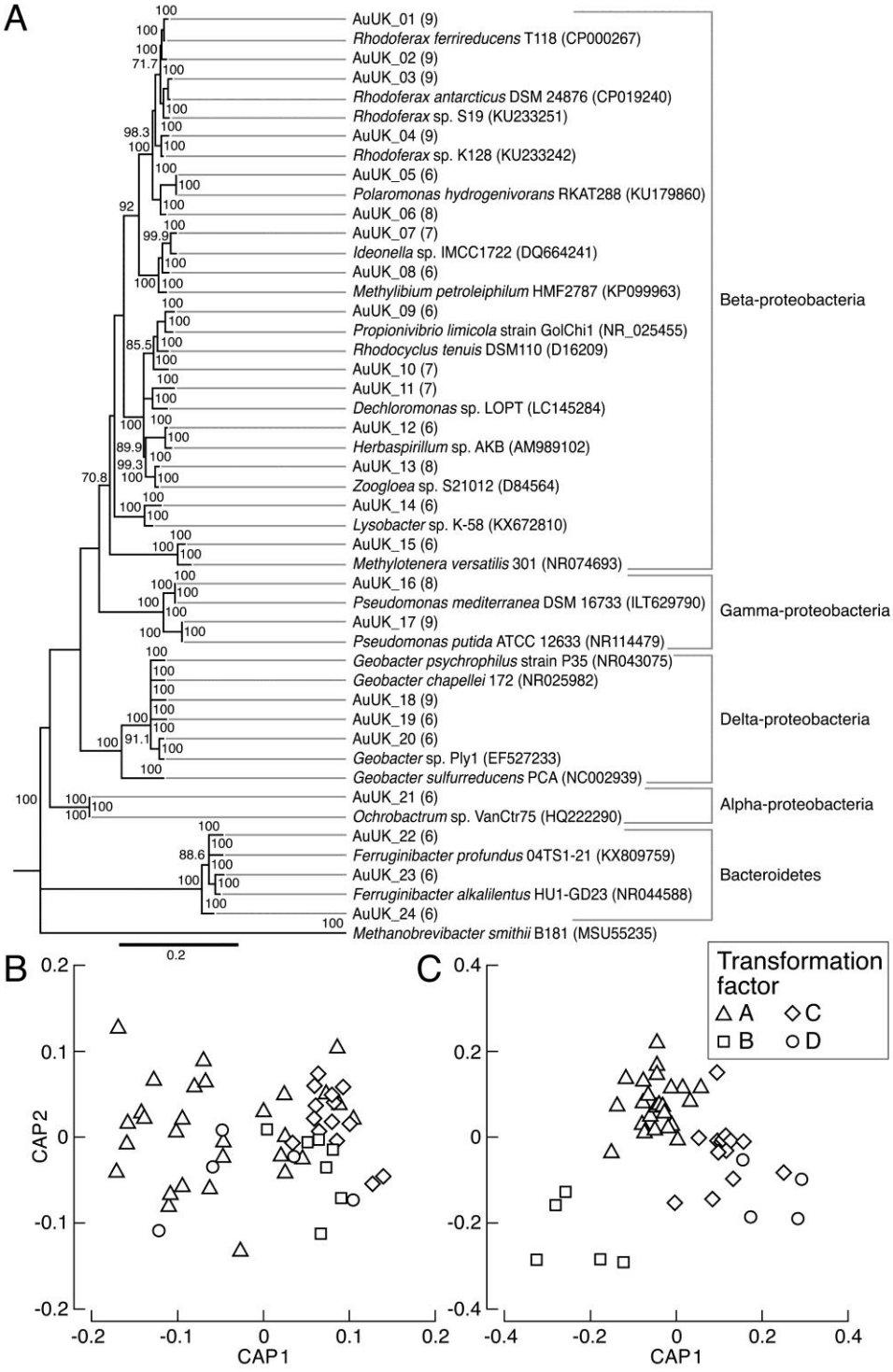

Figure 7 **(A)** A neighbour-joining phylogenetic tree of representative 16S rRNA sequences taxa present on particles from 70 % of the sites. Percentages of 1000 bootstrap values < 70 % are not shown. *Methanobrevibacter smithii* was used as the out-group. The first two canonical axes produced by CAP analyses of **(B)** OTUs in the genus *Rhodoferax* and **(C)** *Geobacter* taxa

analysed for differences in community assemblages in relation to the grade of transformation (TF A to TF D).

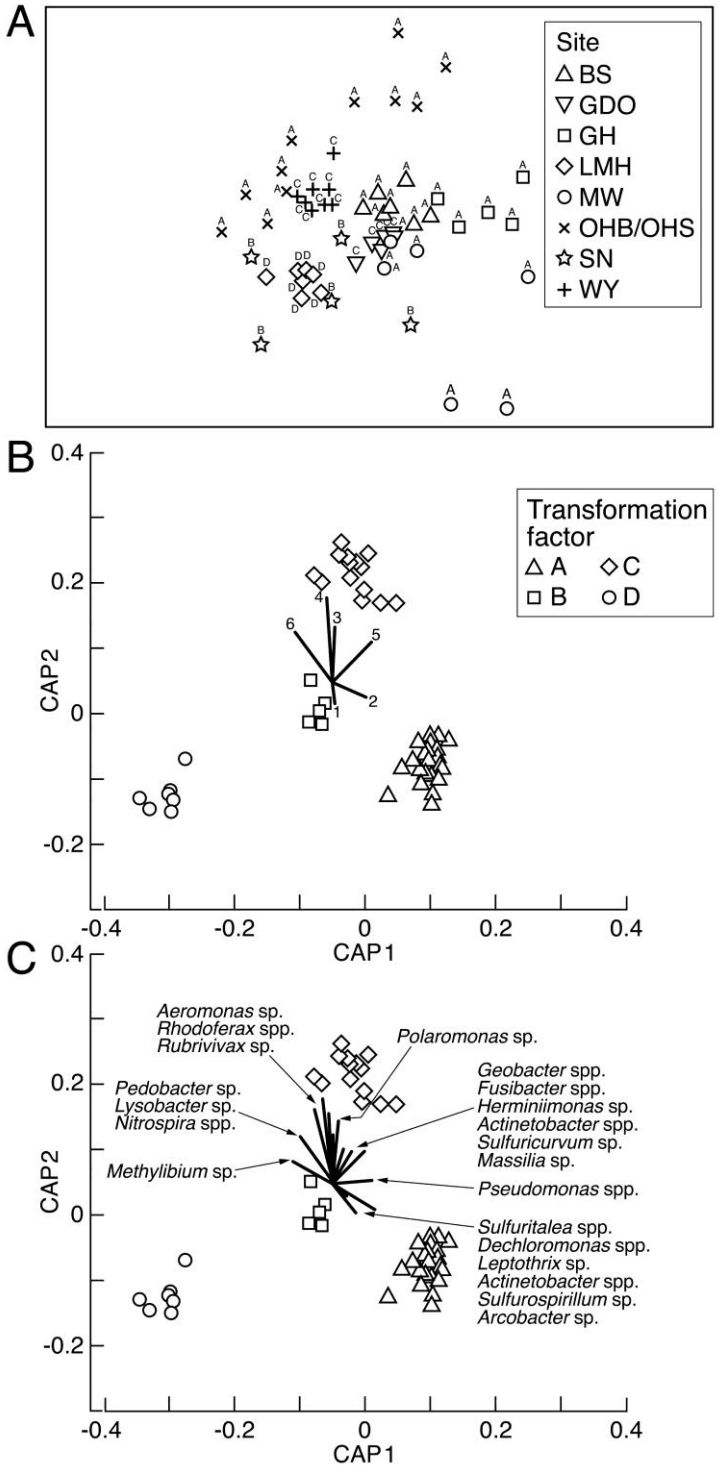

Figure 8 **(A)** A non-metric, multidimensional scaling plot displaying increasing similarities of microbial communities with increasing transformation grade. **(B,**

C) The first two canonical axes produced by CAP analyses based on individual taxa analysed for differences in community assemblages in relation to the grade of transformation (TF A to TF D); vectors of Pearson's correlations **(B)** of assigned biofilm groups 1–6 and **(C)** of taxa with highest %contribution based on SIMPER analysis overlain.

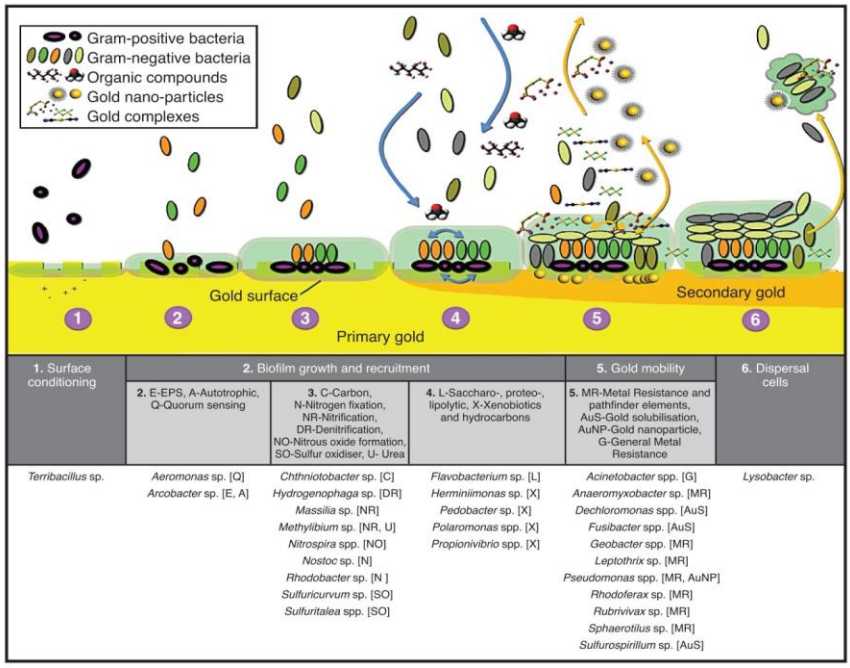

Figure 9 Schematic model and putative functional traits of biofilms on Au-particles from the United Kingdom (modified after Rea, Zammit and Reith 2016): (1) conditioning of surfaces to their attachment; (2) the recruitment of photo- and heterotrophic bacteria; (3–4) the proliferation and growth of the biofilm community including heterotrophic species; (5) the mobilization, detoxification, re-precipitation and utilization of Au by metallophillic species; and (6) the seeding of dispersal cells with release of nano-particle and Au complexes. Functional assignment of OTUs to the six groups are listed in their corresponding columns.